Pergamon

PII: S0967-0645(96)00050-1

Deep-Sea Research II, Vol. 43, No. 7-8, pp. 1601-1625, 1996

0967-0645/96 $15.00 + 0.00

Spatial variability in zooplankton abundance near feeding right whales in the Great South Channel

ROBERT C. BEARDSLEY,* ARI W. EPSTEIN,† CHANGSHENG CHEN,‡
KAREN F. WISHNER,§ MICHAEL C. MACAULAY¶
and ROBERT D. KENNEY§

(*Received* 29 *September* 1994; *in revised form* 1 *February* 1996; *accepted* 14 *May* 1996)

Abstract—On 3 June 1989, during SCOPEX'89, two right whales were observed to be feeding close to the surface at separate sites in the Great South Channel of the Gulf of Maine. The R.V. *Marlin* deployed and monitored a radio tag on one whale, and underway measurements were made near each whale from the R.V. *Endeavor* to investigate the small-scale spatial structure of water properties and zooplankton abundance in the upper water column near the whales. These measurements included two CTD tow-yos, zooplankton sampling with a MOCNESS, continuous vertical profiling of currents with a 150-kHz ADCP, and continuous vertical profiling of zooplankton concentration with a towed acoustic profiler operating at 120 and 200 kHz.

The whales were feeding on a relatively homogeneous mixture of primarily two stages (copepodite IV and V) of a single copepod species (*Calanus finmarchicus*), which was most abundant in the upper 10–20 m of the water column above the seasonal pycnocline. Descriptions of the spatial structure of copepod abundance in patches traversed by the whales were developed based on MOCNESS samples, acoustic backscatter, and light transmission. In particular, a high correlation was found between MOCNESS biomass measurements and certain 200-kHz acoustic biomass estimates, which enabled the acoustic data to be interpreted solely in terms of copepod abundance. Acoustic measurements made in a copepod patch while closely following one whale indicated mean and peak copepod biomasses of 6.0 and 28.4 g m^{-3} (corresponding to mean and peak concentrations of 8.7×10^3 and 4.1×10^4 copepods m^{-3}) in the 4–10 m depth band, where the whale was probably feeding. With a mean energy content of 10^{-3} kcal $copepod^{-1}$, that whale's mean energy intake rate was 3.8×10^4 kcal h^{-1}. The whale was observed to reverse course and turn back into the patch when it swam into a region of lower copepod abundance, with biomass less than roughly 1–3 g m^{-3} or $1.5–4.5 \times 10^3$ copepods m^{-3}. This concentration is consistent with independent estimates of the minimum prey concentration required for a right whale to regain the energy it expends when it feeds.

The next morning, one of the whales was found to be skim-feeding on a *Calanus finmarchicus* patch in which a bucket sample gave a copepod biomass of 256 g m^{-3} or 3.3×10^5 copepods m^{-3}. If this one sample approximated the mean abundance of the patch, then the whale had a mean energy intake of 1.4×10^5 kcal h^{-1}. At this rate, it could consume its daily basal metabolic energy requirement in roughly 9 min, and its annual requirement in roughly two days (assuming continuous feeding at a mean speed of 1.2 m s^{-1} as determined from the ADCP measurements). Although physical advection on regional and smaller scales appears to be an important element in the processes that cause such dense patches to form in this region during late spring, the lack of a clear linkage between the small-scale physical and biological data reported here suggest that some nonphysical, species-

* Department of Physical Oceanography, Woods Hole Oceanographic Institution, Woods Hole, MA 02543, U.S.A.

† WHOI/MIT Joint Program, Woods Hole Oceanographic Institution, Woods Hole, MA 02543, U.S.A.

‡ Department of Marine Sciences, University of Georgia, Athens, GA 30602–2206, U.S.A.

§ Graduate School of Oceanography, University of Rhode Island, Narragansett, RI 02882–1197, U.S.A.

¶ Applied Physics Laboratory, University of Washington, Seattle, WA 98195, U.S.A.

specific animal behavior like swarming must be partially responsible for creating the very densest copepod patches observed during SCOPEX'89.

INTRODUCTION

The primary food of the North Atlantic right whale, *Eubalaena glacialis*, in the North Atlantic is the copepod *Calanus finmarchicus* (Matthews, 1938; Tomlin, 1957; Omura *et al.*, 1969; Nemoto, 1970; Watkins and Schevill, 1976, 1979; Scott *et al.*, 1985; Kenney *et al.*, 1986; Gaskin, 1987, 1991; Wishner *et al.*, 1988; Murison and Gaskin, 1989; Mayo and Marx, 1990). This copepod overwinters in a dormant stage (primarily copepodite V) throughout the western Gulf of Maine, especially in the deep basins, and matures and reproduces in early spring. The young develop during the onset of the seasonal thermocline and the spring phytoplankton bloom into late-stage copepodites and adults by late spring.

Right whales feed by swimming with their mouths open, using their baleen to filter prey out of the water (Nemoto, 1970; Watkins and Schevill, 1976, 1979; Pivorunas, 1979; Mayo and Marx, 1990). This process requires more energy than the whale would expend by swimming with its mouth closed because of the additional drag. In menhaden, a planktivorous fish that feeds in a similar fashion, the energy cost of mouth-open swimming is about 2.5 times that of swimming with the mouth closed at the same speed (Durbin and Durbin, 1983). Since the number of copepods consumed per unit time (and hence the amount of energy available in the form of food) varies with the concentration of copepods in the water, there must be some minimum or threshold concentration of copepods below which it is not energetically favorable for the whale to feed. Mayo and Goldman (1992) estimate this threshold concentration to be 4×10^3 copepods m^{-3}, within the range of peak concentrations detected in the Gulf of Maine, but 1–2 orders of magnitude greater than many of the other samples of copepods collected from various locations in the Gulf of Maine in late spring. This threshold concentration, moreover, represents merely a break-even point: the point at which the whale gains energy, rather than losing it, by attempting to feed. In order to maintain itself, the whale requires more than this break-even concentration. Analysis by Kenney *et al.* (1986), based on standard mammalian metabolic models and copepod energy density values from Comita *et al.* (1966) and Cetacean and Turtle Assessment Program (1982), suggests that the whale must *routinely* feed in patches containing concentrations between 3×10^5 and 1×10^6 copepods m^{-3} in order to *survive*. For physical and biological reasons that are not well understood, extremely dense aggregations of late stage *Calanus finmarchicus* (which have nearly the maximum food value for the right whale) occur in the northern Great South Channel (GSC) region of the western Gulf of Maine in late spring (Wishner *et al.*, 1988, 1995), making it an ideal feeding ground. It is thus not surprising that each spring a large fraction, perhaps the majority, of the western North Atlantic right whale population (estimated at between 300 and 350 individuals) migrates to this region to feed (Kenney *et al.*, 1995).

The South Channel Ocean Productivity Experiment (SCOPEX) was conducted in the spring of 1988 and 1989 in part to identify and study the physical and biological processes that help create and sustain these dense patches of zooplankton, and to observe the behavior of right whales in the Great South Channel and relate it to the distribution of their prey organisms during this period (Kenney and Wishner, 1995). The main 1989 field program (SCOPEX'89) involved two research vessels (the *Marlin* and the *Endeavor*) and an aircraft. The aircraft was used primarily to locate right whales in the GSC area and to provide a

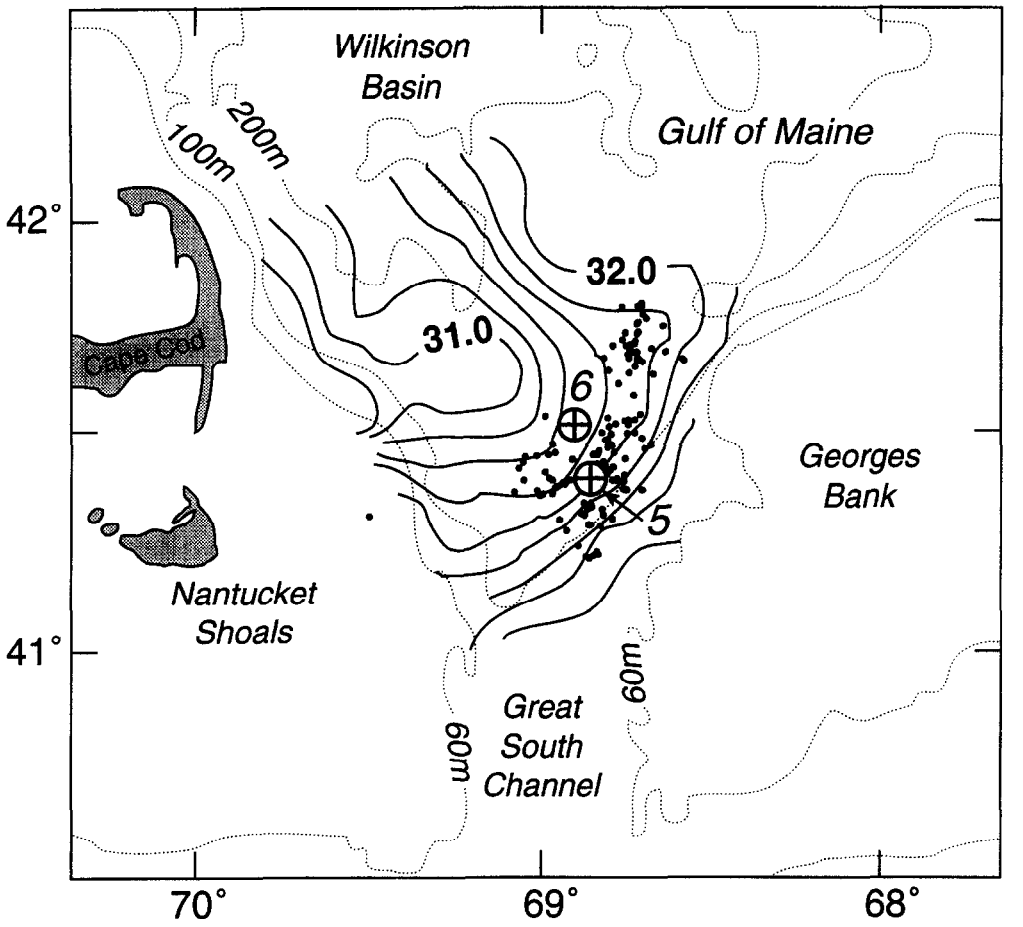

Fig. 1. Map of the Great South Channel region, showing the near-surface (2 m) salinity pattern observed during 6–12 June 1989 and the distribution of right whale sightings (solid dots) made during the three week period 22 May–11 June 1989. Note how almost all the whale sightings are clustered in the leading front associated with the low-salinity plume moving east from Cape Cod. The two circled crosses show the locations of tow-yos 5 and 6, where the observations around feeding right whales on 3 and 4 June described in this paper were made. The 60, 100, and 200 m isobaths are shown for reference. This figure is adapted from Chen *et al.* (1995a) and Kenney *et al.* (1995).

synoptic view of the distribution and abundance of whales in the broader region, the *Marlin* was used for a detailed study of the whales' behavior, and the *Endeavor* was used to make environmental measurements both near the whales and on larger scales within the GSC.

SCOPEX'89 was conducted during May and June of 1989. A series of small-scale physical/biological surveys, diel stations, and other studies were made between 18 May and 6 June, followed by a regional CTD/ADCP survey to determine the larger-scale circulation and water-property structure in the northern GSC. This survey showed that by early June of 1989, the near-surface plume of relatively fresh water normally found each spring off Cape Cod had pushed east, far into the northern GSC (Fig. 1) (Chen *et al.*, 1995a, 1995b). The majority of right-whale sightings during this period occurred in the eastern frontal zone of this plume, where the densest aggregations of late-stage *Calanus finmarchicus* also were

observed (Wishner *et al.*, 1995; Kenney *et al.*, 1995). We present here a description and synthesis of the observations made near two of these whales.

The observations we describe here consist of a combined CTD tow-yo and MOCNESS and acoustic tow made during the late afternoon of 3 June while following one whale; a similar combined tow-yo and tow made that evening while following a second whale; visual, ADCP and radio-tag observations made overnight while attempting to maintain a position near the second whale; and the results of a surface bucket-sample made near that whale the next morning (4 June).

METHODS

Sampling program

A timetable of observations and ship movements on 3–4 June is given in Table 1. The first tow-yo we discuss, which we shall refer to as "tow-yo 5", was made while *Endeavor* followed about 200 m behind a right whale that we shall call "Whale A". This tow-yo, which began at 16:15 h local time (EDT), consisted of two legs. The first leg was made concurrently with a MOCNESS tow (which we refer to as "MOCNESS 43") while the *Endeavor* steamed southward, following the whale as it fed on a large patch of *Calanus finmarchicus*. At 17:10 h, Whale A appeared to reach the edge of the patch and reversed course. After completing MOCNESS 43 and passing out of the patch, the *Endeavor* also reversed course and began leg 2, steaming northward, again following Whale A. Leg 2 was completed at 18:15 h.

At 16:14 h, while *Endeavor* was engaged in tow-yo 5, the *Marlin*, at that time about 14 km west-northwest of *Endeavor*, sighted a right whale known as "Stars", one of the best known individuals in the population. At that time Stars, an 8-year-old female approximately 11–12 m long (New England Aquarium right whale photo-identification catalog data: A. R. Knowlton, personal communication, 1994), was easily recognizable by, among other features, a length of rope entangled in her baleen. Observers on the *Marlin* noted large numbers of copepods and krill visible near the surface. Stars was observed to be actively feeding at and just below the surface, with her open mouth clearly visible. In addition, there were at least three sei whales (*Balaenoptera borealis*), planktivores whose prey preferences overlap those of right whales, feeding in the immediate vicinity. *Marlin* informed *Endeavor* of its observations by radio, and at 16:43 h attached a subcutaneous VHF radio tag, deployed via crossbow, to Stars in order to monitor her movement and surfacing behaviors (Winn *et al.*, 1995). When *Endeavor* had completed tow-yo 5, it steamed toward *Marlin* and Stars, arriving within sight of Stars at about 19:40 h.

The two ships then steamed slowly together, following Stars. A schematic of the *Marlin* and the *Endeavor* with acoustic fin, CTD, and MOCNESS simultaneously deployed while following Stars is shown in Fig. 2. At 20:15 h (approximately sundown), the *Endeavor* began a combined CTD tow-yo, which we refer to as "tow-yo 6", and shallow (0–5 m) horizontal MOCNESS tow (MOCNESS 44) following Stars. At 20:43 h, the *Endeavor* completed MOCNESS 44 but continued the CTD tow-yo following Stars. At 21:00 h, *Marlin* departed for port, still monitoring the radio tag attached to Stars, and at 21:43 h *Marlin* ceased monitoring. Using separate equipment, *Endeavor* continued monitoring the tag. At about 22:30 h, *Endeavor* completed tow-yo 6, made one vertically stratified MOCNESS tow (MOCNESS 45) to the bottom near Stars (actual distance is not known because the whale

Table 1. *Timetable of observations made near right whales during* 3–4 *June* 1989. *Local time is Eastern Daylight Time (EDT), which differs from Greenwich Mean Time (GMT) by* 4 h *(GMT = EDT* + 4 h)

Date	Time	Description of Activity
3 June	14:00	*Endeavor* rendezvous with *Marlin* near 41.4°N, 68.8°W.
	14:29	*Endeavor* starts sampling near Whale A with acoustic fin.
	16:15	*Endeavor* starts tow-yo 5 Leg 1 (CTD 139) and shallow MOCNESS 43 following feeding Whale A.
	16:43	*Marlin* deploys radio tag on Stars, begins monitoring dive time.
	16:56	*Endeavor* finishes Leg 1 of tow-yo 5, MOCNESS 43.
	17:15	*Marlin* starts zooplankton tow near Stars.
	17:17	*Endeavor* starts Leg 2 of tow-yo 5.
	18:15	*Endeavor* finishes Leg 2 of tow-yo 5, steams northwest toward *Marlin* and Stars.
	19:40	*Endeavor* makes visual contact with Stars.
	19:45–21:00	Ships steam together behind or near Stars.
	20:15	*Endeavor* starts tow-yo 6 (CTD 140) and shallow MOCNESS 44 following Stars (feeding).
	20:20	Behavior of Stars begins to change. Eventually she becomes nearly motionless at the surface (and perhaps asleep).
	20:43	*Endeavor* finishes MOCNESS 44.
	20:45	Stars rests at surface for 6.47 min.
	21:00	*Marlin* departs for home, continues to monitor radio tag.
	21:43	*Marlin* stops monitoring radio tag.
	22:27	*Endeavor* finishes tow-yo 6.
	23:23	*Endeavor* starts deep MOCNESS 45.
	23:55	*Endeavor* finishes MOCNESS 45, continues tracking Stars by radio (with limited success) through the night.
4 June	04:07	Stars passes within about 100 m of *Endeavor*.
	05:23	*Endeavor* sights Stars skim-feeding near the surface; *Endeavor* begins following Stars closely as she feeds.
	07:50	*Endeavor* takes 10 liter surface bucket sample near Stars.
	08:20	*Endeavor* takes XBT 12 near Stars.
	08:36	*Endeavor* loses sight of Stars.
	09:00	Dense fog rolls in, making further visual tracking impossible.
	09:00–11:30	*Endeavor* receives only intermittent signals from radio tag; no good data recorded.
	11:30	*Endeavor* departs for next work area.

could not be seen in the dark, but relative closeness (within 1–2 km) was estimated based on the intensity of signals received from the radio tag), and then spent the rest of the night attempting to track Stars via the radio tag (with only partial success). At 05:23 h the next morning (sunrise occurred at 05:08 h), Stars was observed skim-feeding in a large *Calanus* patch near 41.4°N, 68.9°W. At 07:50 h, *Endeavor* took a surface bucket sample to measure the zooplankton concentration in this patch. Visual contact with Stars was lost at 08:36 h, and at about 09:00 h a dense fog rolled in, making further visual tracking impossible. Reception of the tag's radio signals became poor and intermittent, and at about 11:30 h *Endeavor* left the area to conduct other studies.

Instrumentation and data processing

Measurements made during tow-yos 5 and 6 included: (i) hydrographic and current profiling with the *Endeavor*'s NBIS Mark III CTD and 150-kHz RDI acoustic Doppler

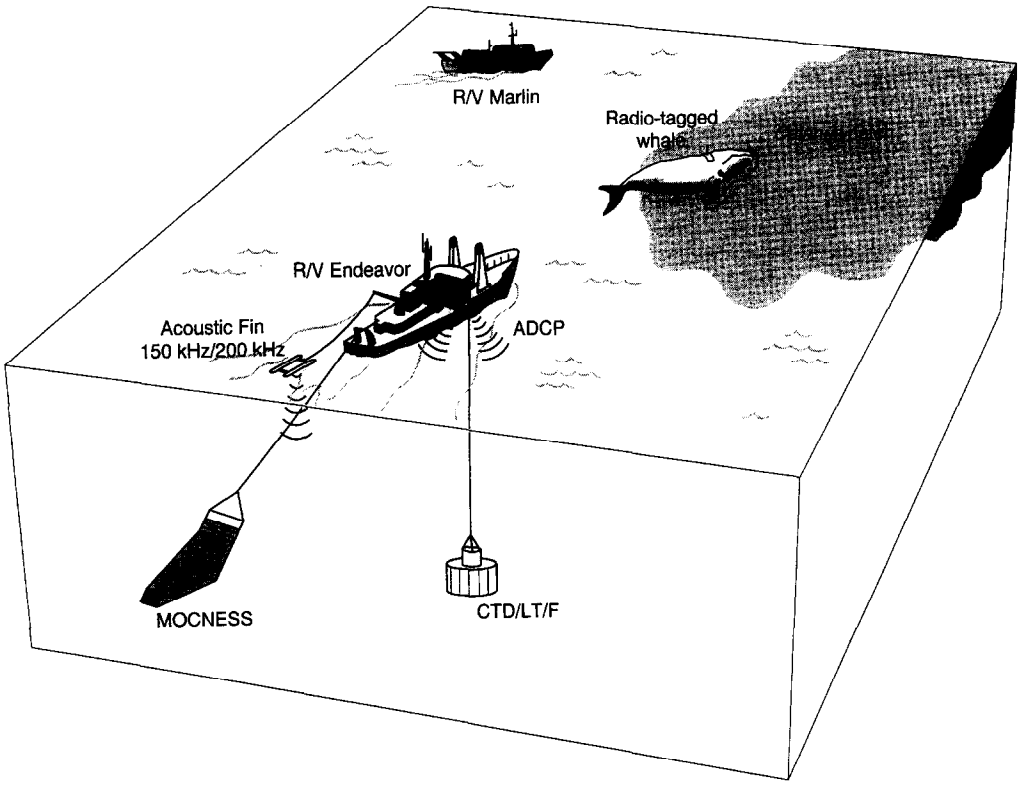

Fig. 2. Schematic showing the *Marlin* and *Endeavor* sampling around the right whale Stars during tow-yo 6 on 3 June 1989. The *Endeavor* made simultaneous measurements with a CTD/light-transmission/fluorometer profiler, a towed dual-frequency acoustic profiler, MOCNESS, and the ship's ADCP. The *Marlin* observed the whale's eating and diving behavior both visually and by monitoring a VHF radio tag.

current profiler (ADCP), respectively; (ii) biological sampling with MOCNESS [a multiple opening and closing net and environmental sampling system (Wiebe *et al.*, 1976, 1985)] and other towed nets (Wishner *et al.*, 1995); and (iii) acoustic profiling for zooplankton distribution and biomass with a towed Biosonics Model 101 120- and 200-kHz acoustic fin (Macaulay *et al.*, 1995). The CTD was equipped with a Sea Tech 25-cm pathlength transmissometer and Sea Tech fluorometer, and it was rigged with a simple steering vane attached to the rosette sampler in order to keep the sensors oriented into the flow. The CTD was lowered off the starboard side and yo-yoed between about 2 m and 60 m every 6 min with a lowering speed of about 20 m min^{-1}. Only the downcast data were analyzed. The 1 m^2 MOCNESS (with nine 335-μm mesh nets) was deployed over the stem and towed at about 1.5 kt (0.83 m s^{-1}) to maintain the optimal 45° net angle. About 130 m^3 of water were filtered through each MOCNESS net. The acoustic fin was towed off the port stern quarter at a depth of 0.5–1.0 m, and useful acoustic data were generally obtained at depths deeper than about 4 m.

One objective of sampling the zooplankton distribution around Whale A and Stars with acoustics and the MOCNESS simultaneously was to intercalibrate these techniques, so that

if they provided good quantitative agreement, the acoustics could be used to obtain a continuous, high-resolution record of zooplankton abundance over time and space. The acoustic data were recorded in several formats. The 120- and 200-kHz data were processed separately on a PC into biomass estimates, averaging over 60-s × 1-m blocks, and recorded on disk. Some of this information was also displayed in real time aboard ship in order to help monitor and direct the ongoing sampling. During leg 1 of tow-yo 5, some raw 200-kHz acoustic data were also recorded digitally for backup. After the 1989 field work was completed, the Biosonics unit was calibrated at the University of Washington Applied Physics Laboratory. The raw 200-kHz data from tow-yo 5 were then processed into biomass estimates, averaging over 30-s × 1-m blocks, using optimum threshold and gain settings. Copepod biomass was computed using a conversion factor of -36 db kg^{-1}, based on previous work [see Macaulay *et al.* (1995) for more details about the acoustic system and data processing].

We found in subsequent analysis that only the 30 s, 200 kHz data provided good quantitative estimates of copepod biomass. The 60 s, 200 kHz data provided a useful qualitative picture of the vertical distribution of copepods and larger zooplankton (which were also observed in the 60 s, 120 kHz data), but the estimates of copepod biomass were reduced in places where the abundance of individuals was insufficient to produce measurable scatter (see Macaulay *et al.*, 1995). As a result, only the limited time series of 30 s, 200 kHz data taken during tow-yo 5 was used to intercalibrate with MOCNESS-derived biomass estimates. Details of the comparison between 200-kHz acoustic data and MOCNESS biomass estimates are given in Appendix A.

During tow-yos 5 and 6, we noticed extreme "noise", or scatter, in the profiles of light transmission made by the CTD. This scatter had a distinctive feature: the maximum values of light transmission (plotted versus depth) seemed to follow a relatively smooth curve, but in many depth ranges, lower values of transmission seemed to be scattered randomly below that maximum. In the regions of high scatter, consecutive measurements of light transmission often differed greatly. This pattern suggested that the scatter was due not to changes in the amount of small particulate matter in the water, but rather to intermittent appearances of relatively large obstructions. Further analysis, described in Appendix B, showed that this scatter was strongest in regions of high copepod concentration (as measured by the 200-kHz acoustic data). We believe that the presence of the copepods themselves is responsible for scatter in the transmissometer data: that is, that the light transmission was noticeably reduced when one or more copepods moved through the beam. As discussed in Appendix B, copepod concentrations were high enough during tow-yos 5 and 6 to cause the observed scatter. Since light-transmission data were collected on each CTD cast during each tow-yo, we can use the light-transmission data to crudely map the copepod distribution during the tow-yos, even for those times when acoustic data are not available.

RESULTS

Tow-yo 5

As mentioned above, tow-yo 5 consisted of two legs, the first made following Whale A southward as it fed on a large patch of *Calanus finmarchicus* and the second made following the whale as it reversed course to turn back into the patch and continue feeding. During

leg 1, both 30 s, 200 kHz acoustic and MOCNESS 43 biomass data were collected, and the composite picture shown in Fig. 3A provides our best description of the spatial structure of zooplankton near a feeding right whale. The qualitative agreement between acoustic biomass and rms light-transmission deviation shown in Fig. 3B (see Appendix B) makes it possible to use transmissometer data to get a crude idea of the copepod distribution during the rest of tow-yo 5, for which 30 s, 200 kHz acoustic data do not exist. Figure 4 shows rms light-transmission deviation for all of tow-yo 5, with isopycnal surfaces shown superimposed. The break in the CTD casts between casts 9 and 10 (around 2500–3100 m along the transect) corresponds to the period when the ship reversed course between legs 1 and 2. The deeper, lightly shaded areas represent dense patches of larger zooplankton (presumably euphausiids) detected in both the 120 and 200 kHz acoustic data (Macaulay *et al.*, 1995). These deeper patches were part of a dense layer of larger zooplankton that rose from near the bottom towards the surface during the day.

The combined picture of zooplankton distribution shown in Figs 3 and 4 indicates a thick layer of copepods extending down to about 15 m at the start of leg 1. This layer then seems to become thinner, extending down to only about 6–7 m, and the copepod concentration seems to decrease (as measured by the intensity of the rms transmissometer deviation and decrease in MOCNESS concentration) towards the end of leg 1. This thinning and weakening of the copepod layer corresponds roughly to the region (estimated uncertainty 200 m) where Whale A ceased feeding and reversed direction. During leg 2, which corresponds roughly to the region (estimated uncertainty 400 m) where the whale began feeding again, the copepod layer at first seems very weak, but gradually builds in intensity and remains near-surface. Since the top 3–4 m were not sampled by either acoustics or CTD during tow-yo 5, only the observation that Whale A was not skim-feeding indicates that the maximum copepod concentrations occurred beneath the top 0–1 m.

The distribution of copepods within this near-surface layer was clearly patchy, both horizontally and vertically. The horizontal average of the 30 s, 200 kHz acoustic biomass data shown in Fig. 3A over a distance of about 1.5 km did not vary much with depth between the top depth sampled (about 4.1 m) and 10 m, and had a mean value of about 6.0 g m^{-3} over this depth band. Based on MOCNESS 43 results (Table 2), the average copepod wet weight was 0.69 ± 0.18 mg, so that the spatial mean concentration in the 4–10 m depth band was 8.7×10^3 copepods m^{-3}. Short gaps in the copepod layer occurred

Fig. 3. (A) Contour plot of the 30 s, 200 kHz acoustic biomass field for the first part of leg 1 of tow-yo 5. Although good data were collected to near the bottom, only acoustic data in the upper 25 m are displayed here, since the copepod layer was confined to the top 10–20 m. The contour values (1, 5, 9, 13, 17, 21, and 25 g m^{-3}) were chosen to highlight the copepod biomass distribution. Biomass values above 25 g m^{-3} are not contoured but shown in gray; these larger values correspond to the layer of larger zooplankton (presumably euphasiids) and some individual fish located below the copepod layer. Note that no acoustic data were collected in the top 4.1 m, causing the blanking of that layer. Also no data were collected between 25 and 150 m along the transect. The vertical dashed lines indicate the locations of CTD stations 1–6. Superimposed is the smoothed trajectory of MOCNESS 43, with nets 2 and 9 marked. This path has been shifted in time and depth to give the best correlation between the acoustic and MOCNESS biomass estimates: the path shown is the optimum one, giving a correlation coefficient of 0.971. (The depth of both acoustic and MOCNESS data has also been shifted to give the best correlation between acoustic and light-transmission data, see Appendix A.) (B) Comparison of the per cent rms light transmission deviation profiles with acoustic biomass profiles measured along the dashed lines shown above in (A). The relative depth of the acoustic data has been shifted vertically to give the best correlation of the landmark depths shown in Fig. B3.

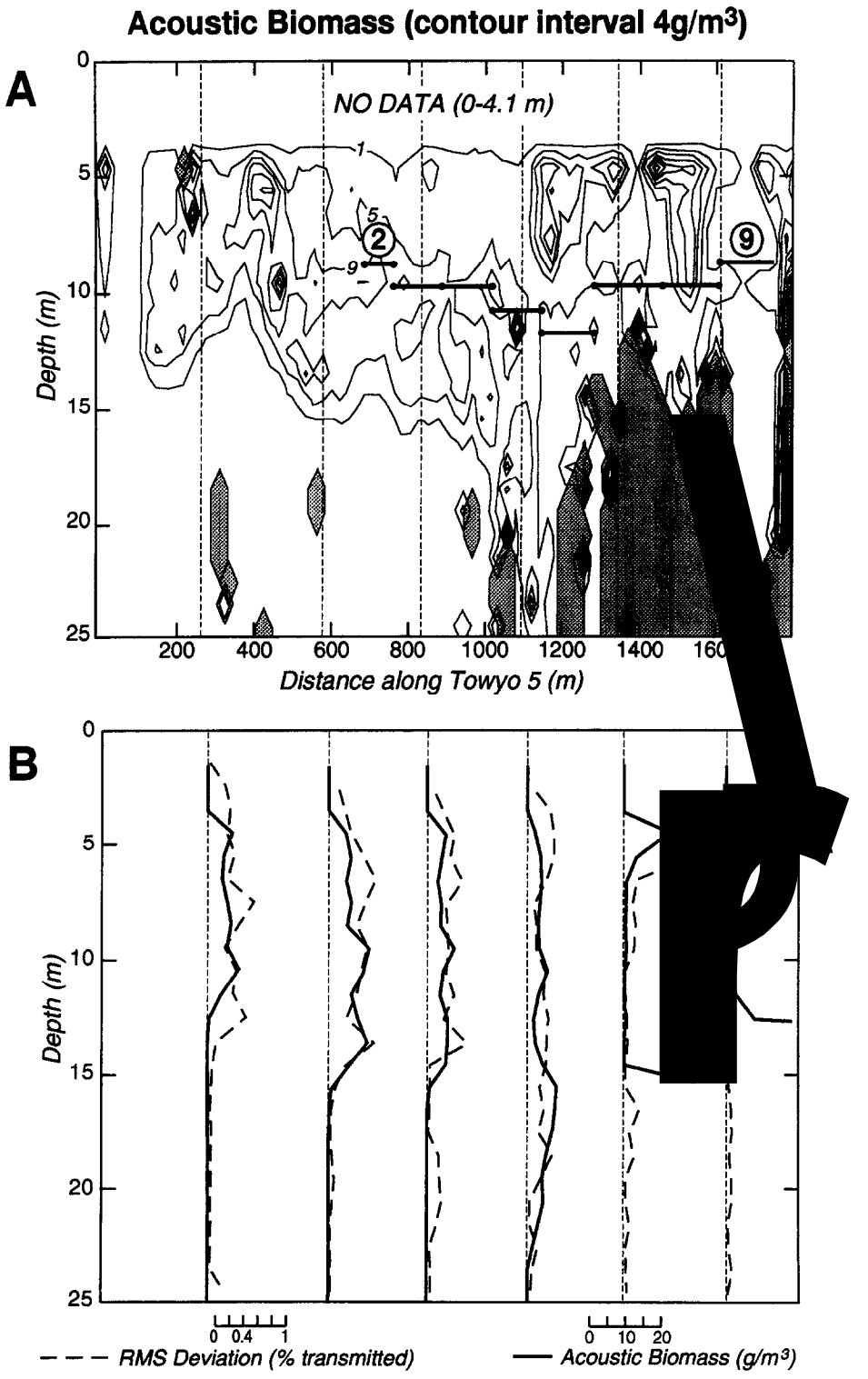
Acoustic Biomass (contour interval 4g/m3)
A
NO DATA (0-4.1 m)
Depth (m)
Distance along Towyo 5 (m)
B
Depth (m)
0 0.4 1
RMS Deviation (% transmitted)
0 10 20
Acoustic Biomass (g/m3)

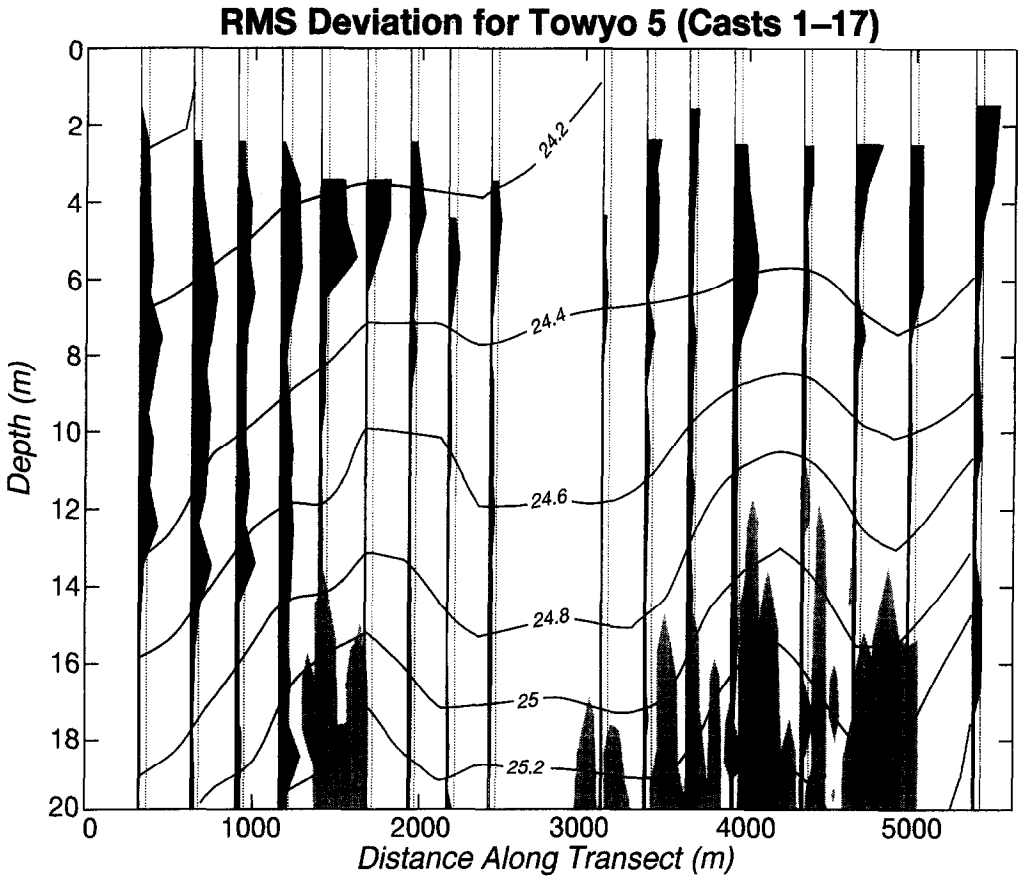

Fig. 4. Profiles of per cent rms light-transmission deviation plotted as a function of position along the entire tow-yo 5 transect. The dark shaded areas indicate the per cent rms deviation measured during each CTD lowering while the lighter shaded areas denote regions where large (non-copepod) zooplankton were found in the acoustic data. Dotted lines indicate an rms deviation of 0.2% transmission, the level below which light-transmission estimates of copepod biomass are essentially indistinguishable from zero due to curvature of the "background" light-transmission curve. Superimposed are isopycnals spanning the range of σ_t from 24.0 to 25.4. The σ_t labels appear in the gap separating leg 1 from leg 2.

near 1400 and 1650 m, creating one almost discrete patch roughly 250 m long with mean and maximum biomass estimates of 7.7 and 28.4 g m^{-3}, which correspond roughly to mean and peak concentrations of 1.1×10^4 and 4.1×10^4 copepods m^{-3}, respectively. Although the acoustic approach may underestimate the larger biomass values (Appendix A), the acoustic peak concentration of 4.1×10^4 copepods m^{-3}, observed at a depth of 4 m at 1450 m, is about twice the peak concentration of 2.4×10^4 copepods m^{-3} found in MOCNESS 43 (Table 2). This difference is due to both the longer horizontal sampling distance of the MOCNESS and to its ability to sample only one depth interval at a time.

The top 4–30 m of the water column was strongly stratified during tow-yo 5 (Fig. 4). Salinity and temperature contributed roughly equally to the formation of the pycnocline, with the maximum vertical density gradient occurring between 12 and 20 m on average. The maximum spatially averaged Brunt Väisälä frequency was $N_{max} \cong 2.3 \times 10^{-2}$ s^{-1}. There

Table 2. Results of the MOCNESS and bucket samples taken around two feeding right whales during 3–4 June 1989. The time of sampling is listed in column 1. The volume filtered was determined from a flowmeter attached to the MOCNESS frame; no attempt was made to correct for volume bias due to vertical velocity during oblique tows (see Burd and Thomson, 1993), however this should not be a problem during the horizontal tows made during MOCNESS 43 and 44. This table was adapted from Schoenherr and Wishner (1990). CIII+ abundance is the total abundance of all lifestages from CIII to adults. For information on MOCNESS sampling and processing, see Wishner et al. (1995). (Note: In title of last column PTZ = proportion of total zooplankton)

MOC No.	Net No.	Minimum Pres. (dbars)	Maximum Pres. (dbars)	Volume Filtered (m^3)	Total Biomass (mg/m^3)	Copepod Biomass (mg/m^3)	CIII + Abund. ($no./m^3$)	CIII Abund. ($no./m^3$)	CIV Abund. ($no./m^3$)	CV Abund. ($no./m^3$)	*F* Abund. ($no./m^3$)	*M* Abund. ($no./m^3$)	*Cal. finmarchicus* PTZ
43	1	0	10	197.9	11,080	11,080	22,744	497	14,203	8045	0	0	1.00
16:19–	2	8	9	81.2	10,526	10,526	24,434	349	11,344	12,217	349	175	1.00
16:48	3	9	10	121.2	11,045	11,045	12,687	37	6139	6325	149	37	1.00
Tow-yo 5	4	9	10	119.2	8082	8082	12,686	70	6850	5697	70	0	0.99
	5	9	11	129.6	4499	4499	7777	0	3854	3889	35	0	0.99
	6	10	11	138.9	932	932	1525	4	487	1015	11	8	1.00
	7	9	10	166.1	1017	1022	1264	5	263	987	9	0	1.00
	8	8	10	141.4	8342	8342	9343	0	1023	8097	222	0	1.00
	9	8	9	144.3	84	70	98	3	43	51	1	0	0.82
44	1	0	2	151.2	5243	5243	10,804	429	7816	2576	18	0	1.00
20:18–	2	0	2	98.9	8916	8916	15,569	848	11,813	2908	0	0	0.97
20:43	3	0	2	100.0	7918	7918	19,746	849	15,429	3468	0	0	1.00
Tow-yo 6	4	1	2	112.2	6872	6872	14,921	1027	11,297	2598	0	0	0.98
	5	1	5	114.8	7518	7518	18,925	1219	15,012	2694	0	0	0.99
	6	1	5	99.2	4290	4290	12,530	660	9712	2158	0	0	1.00
	7	1	2	100.9	1678	1677	5684	431	4343	894	0	16	1.00
	8	1	4	100.6	2408	2402	6022	723	4204	1095	0	0	1.00
	9	3	5	99.6	3549	3174	7230	738	5295	1197	0	0	1.00
45	2	87	138	202.7	501	452	452	2	114	291	17	27	0.91
23:23–	3	46	86	261.1	197	158	120	0	14	66	35	5	0.79
23:55	4	19	46	123.3	989	868	501	11	219	238	30	4	0.99
(Night)	5	16	19	77.9	1810	1746	2591	25	1917	625	0	25	1.00
	6	12	16	80.8	2262	2193	4546	15	3005	1495	31	0	1.00
	7	7	12	95.9	4730	4684	11,740	1038	9174	1529	0	0	1.00
	8	2	7	76.9	220	115	285	49	189	47	0	1	0.99
	9	0	3	113.7	428	109	253	45	157	52	0	0	0.83
Bucket Sample (07:50)	—	—	—	0.01	256,100	256,100	331,200	3200	180,000	140,000	800	7200	0.99

some shoaling of the near-surface isopycnals with time during tow-yo 5, suggesting that the thinning of the copepod layer during the tow-yo may be associated with the rising density field. There was little evidence of a surface mixed layer, and the copepod layer did extend down through the near-surface stratification, although most of the copepod layer was located above the maximum vertical density gradient. The ADCP velocity data exhibited small but measurable variations (of order 2–7 cm s^{-1}) in both vertical and horizontal directions during tow-yo 5; however, no clear picture of horizontal convergence or vertical shear was found. The average vertical shear squared, S^2, was about 3×10^{-4} s^{-2}, roughly uniform with depth over the top 30 m, such that the local gradient Richardson number $Ri = N^2/S^2$ was generally greater than 0.5, indicating that active vertical mixing was not occurring in the copepod layer.

Tow-yo 6

The start of tow-yo 6 was located about 18.4 km west-northwest from the end of tow-yo 5 and closer to the core of the fresh-water surface plume (Fig. 1). As a result, the near-surface water was fresher, with a layer of relatively constant salinity in the top 5 m. The surface water was stratified in temperature, with both temperature and salinity gradients maximum between about 10 and 18 m on average. The mean density gradient was also a maximum in this depth range (Fig. 5), with a maximum Brunt–Väisälä frequency of $N_{max} \cong 2.7 \times 10^{-2}$ s^{-1}. The average vertical shear squared decreased from about 8×10^{-4} s^{-2} near 9 m (the shallowest depth at which estimates of S can be made) to about 4×10^{-4} s^{-2}, below 14 m. As during tow-yo 5, the local gradient Richardson number was generally greater than 0.5, indicating a lack of active shear-induced mixing.

The MOCNESS sampled the top 5 m of the water column and copepod biomass, and concentrations were similar to those found during tow-yo 5 (Table 2). The rms light-transmission deviation data showed a patchy distribution, with a thick layer of high copepod biomass extending down to a depth of 16 m throughout the tow-yo (Fig. 5). The horizontal structure was also patchy, with maximum rms light-transmission deviations a bit larger than, but comparable to, those found in tow-yo 5.

From the time *Marlin* had first sighted Stars, the whale's behavior had been characterized by a sequence of short dives (15–60 s in duration) and very short surfacings, with occasional dives as long as 2–3 min (Figs 6 and 7). For much of the time she was visible just below the surface, feeding. At about 20:20 h, just after sundown, she began to surface for longer intervals, and at 20:30 h she made the longest dive in the sequence (about 4 min). She then stopped feeding and rested on or very near the surface. In the dim twilight, she could be seen clearly remaining nearly motionless with her back above the surface. Stars and *Marlin* remained in constant relative position to each other as both drifted with the current; during her earlier feeding, in contrast, *Marlin* had needed to engage its propeller frequently, in order to maintain the desired distance from the whale. Winn *et al.* (1995) speculate that Stars may have been sleeping during this quiescent interval. In any case, the light-transmission data indicate that the whale did *not* stop feeding because of a lack of available copepod biomass.

Other observations

Later that night, the *Endeavor* made a bottom-to-surface oblique MOCNESS tow

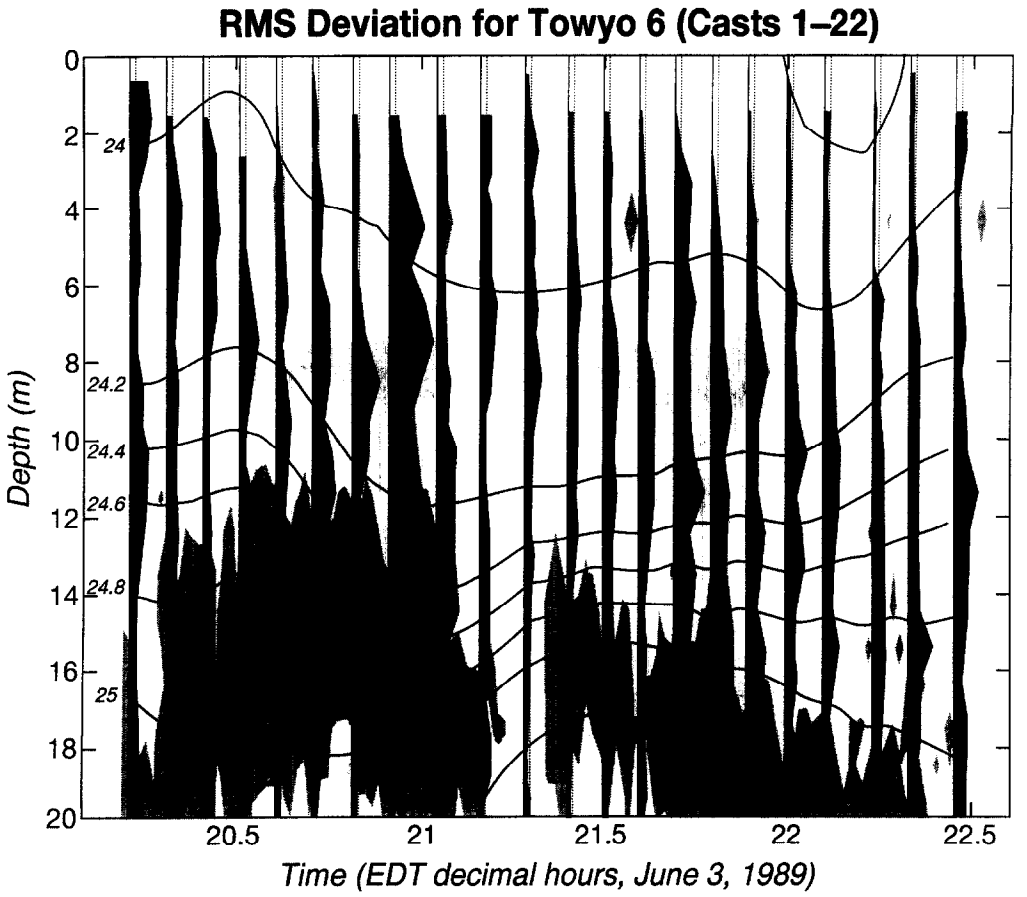

Fig. 5. Profiles of per cent rms light-transmission deviation plotted as a function of time along the entire tow-yo 6 transect. The dark shaded areas indicate the per cent rms deviation measured during each CTD lowering while the lighter shaded areas denote regions where large (non-copepod) zooplankton were found in the acoustic data. Dotted lines indicate an rms deviation of 0.2% transmission, the level below which light-transmission estimates of copepod biomass are indistinguishable from zero. Superimposed are isopycnals spanning the range of σ_t from 24.0 to 25.2. The σ_t labels are shown to the left.

(MOCNESS 45). *Calanus finmarchicus* was found in concentrations above 10^3 copepods m^{-3} only in the top 20 m (Table 2). Other net sampling conducted in this general region during the last week in May and the first week in June 1989 indicated that *Calanus finmarchicus* remained concentrated near the surface and did not exhibit diel vertical migration behavior (Wishner *et al.*, 1995).

Sunrise the next morning was at 05:08 h. At 05:23 h, Stars was observed to be surface-feeding near 41.45°N, 68.96°W, approximately 1.2 km west-southwest of the spot she would have been had the tidal current carried her from the location where she was first sighted by the *Endeavor* (Fig. 8). She was then followed by the *Endeavor* and observed to continue to feed until about 08:36 h when visual contact was lost in fog near 41.51°N, 68.98°W. Stars first swam southward, then turned and swam northward as she was also carried northward

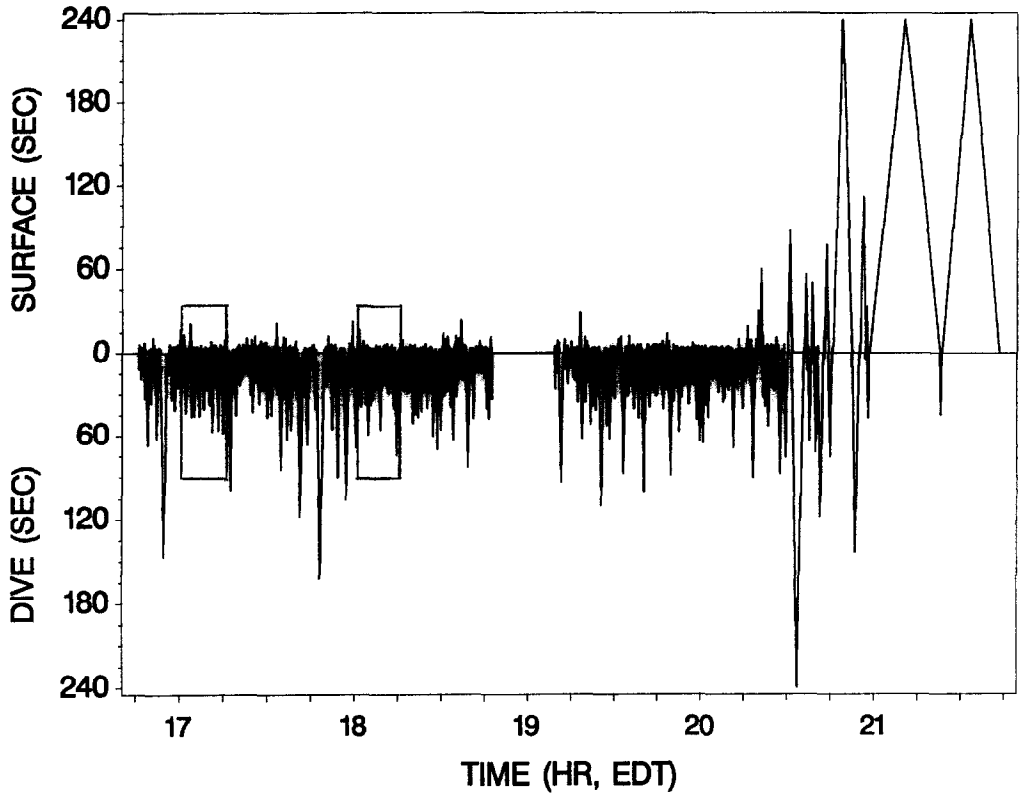

Fig. 6. Detailed surface and dive data for radio-tagged right whale (Stars) on 3 June 1989. Surface durations are shown by upward spikes and dive durations by downward spikes. Both are truncated at 4 min for clarity. The duration of the long dive at approximately 20:35 was 4 min, 12 s. The three long surfacings at the end of the sequence were 6 min, 72 s; 24 min, 24 s; and 19 min, 48 s, respectively. The two boxes represent the segments expanded in Fig. 7. The gap centered near 19:00 indicates when no data were collected.

by the current. The water near the whale was reddish due to high concentrations of *Calanus finmarchicus* very close to the surface. A surface bucket sample taken from the *Endeavor* near the whale had the highest copepod concentration found during SCOPEX'89 (Table 2). The copepod biomass estimate was 256 g m^{-3} and the concentration of CIII and older *Calanus* was 3.3×10^5 copepods m^{-3}, both more than one order of magnitude larger than observed during sampling the previous evening around Stars.

During this period the *Endeavor* steamed slowly behind Stars, attempting to follow her within 0.5 km without influencing her behavior. We have used the *Endeavor* 7-m ADCP data to estimate both Stars' swimming speed while feeding and the size of the *Calanus* patch. Over the 3-h period, the average speed of the *Endeavor* through the water (at 7 m) was 1.22 m s^{-1}. If we neglect vertical shear and assume the uncertainty in relative position between the *Endeavor* and Stars was 0.5 km at each end of the path, the uncertainty in speed would be about 0.1 m s^{-1}. Thus, we estimate that the minimum mean speed of Stars during this feeding period was 1.2 ± 0.1 m s^{-1}. This estimate is within the upper limit of 1.5 m s^{-1} cited by Watkins and Schevill (1979) for right whales in this region. Since Stars was observed

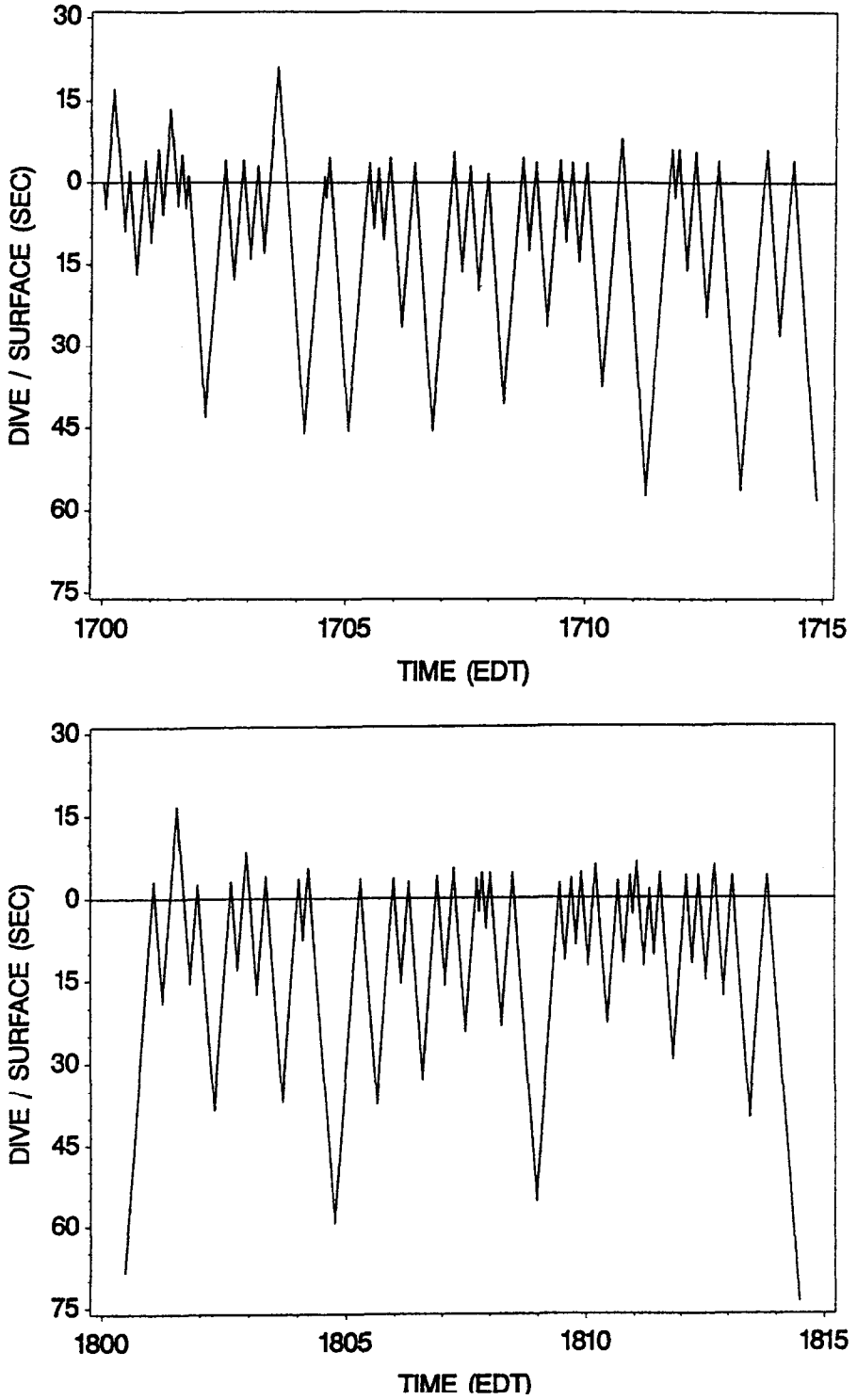

Fig. 7. Expanded 15 min examples of Stars dive and surface data on 3 June 1989.

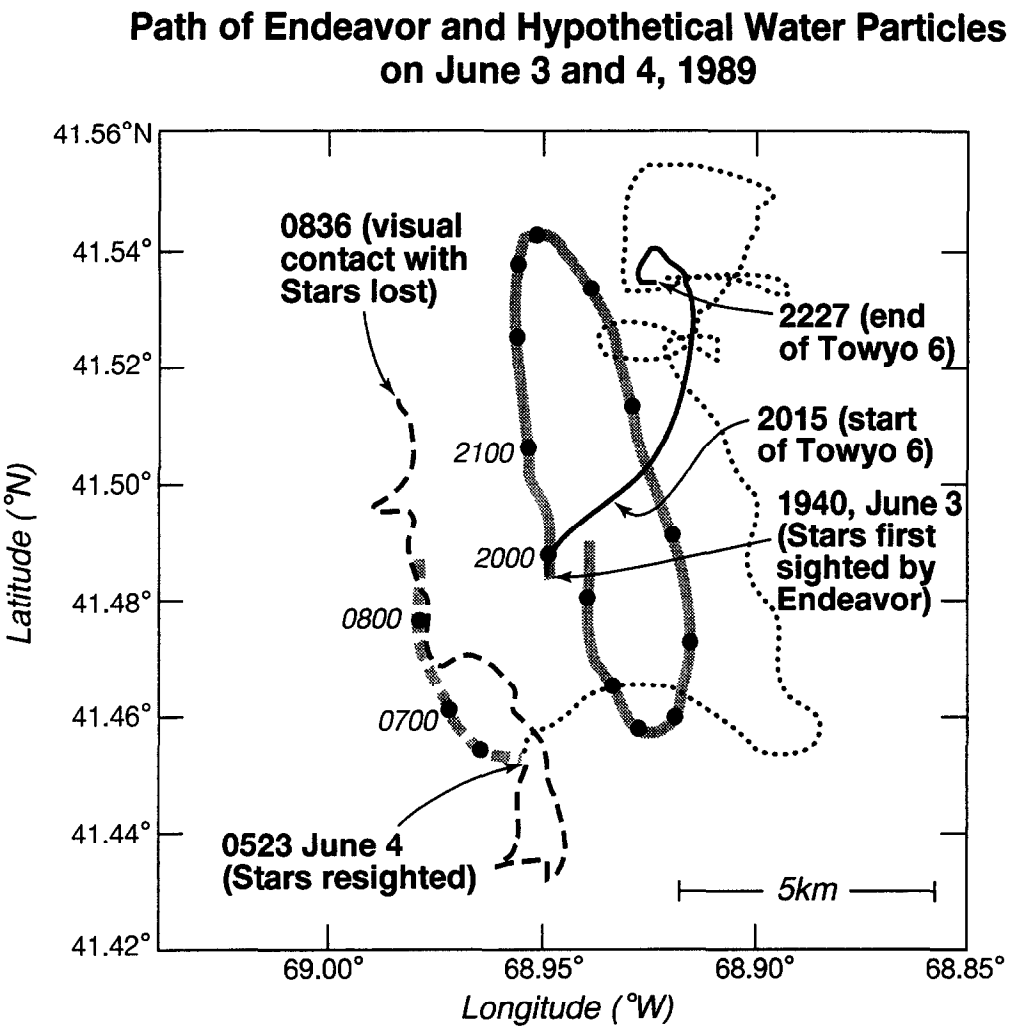

Fig. 8. Map showing path of the R.V. *Endeavor* between 19:40 h on 3 June and 08:35 h on 4 June as it tracked Stars. The path of the *Endeavor* between first sighting Stars at 19:40 and the end of tow-yo 6 at 22:27 is shown as a dark solid curve. A dotted curve is used to show the path as *Endeavor* conducted MOCNESS 45 and attempted to track Stars through the night. At 05:23 4 June, the *Endeavor* spotted Stars again and followed her closely until about 08:36, following the path shown by the dark dashed curve. Also shown are the paths of two hypothetical water particles constructed using the *Endeavor* 7-m ADCP data. The trajectory of the first particle (shown as a broad solid curve) starts at the same location and time where Stars was first sighted on 3 June by *Endeavor*. This particle moves in a elongated elliptical path oriented approximately north–south, indicative of the strong semi-diurnal tidal current in this region. The solid dots along this path indicate a time interval of one hour, with the times of the first two dots given. The second particle starts at the same location and time where Stars was re-sighted on 4 June. Over the approximately 3 h period that Stars was tracked (the time interval between dots is 1 h), this second particle moved northward along its primarily tidal trajectory, shown by a broad dashed curve. It is interesting to note that Stars was spotted at 05:23 h on 4 June only 1.2 km west-southwest from where she would have been carried by the tidal current if she had just floated passively in the water. Earlier that morning at 04:07, her radio tag had been heard from the *Endeavor* just 0.9 km east of where the tidal current would have carried her.

to feed throughout this period, the minimum north–south extent of the surface patch was 5.3 km. We have no knowledge of the east–west extent of the patch.

DISCUSSION

The experimental strategy of using right whales to locate dense patches of their copepod food, *Calanus finmarchicus*, proved successful in SCOPEX'89. On 3 June, two right whales were found feeding near the surface. One whale (Whale A) was followed for about 3 h, and the other (Stars) was tagged with a VHF radio transmitter and subsequently followed for about 16 h, sometimes by a single vessel and sometimes by two vessels working together. Underway measurements were made in order to investigate the small-scale spatial structure of water properties, light transmission, and zooplankton in the upper water column near both whales.

If we take 1–3 g m^{-3} as the minimum copepod biomass detectable with the light-transmission approach (based on Fig. B3C, Appendix B), then during tow-yo 5 Whale A apparently stopped feeding when the concentration dropped below about 1.5–4.5 $\times 10^3$ copepods m^{-3}. This value is consistent with Mayo and Goldman's (1992) estimate that the threshold prey concentration for a right whale (the concentration above which the whale gains more energy by feeding than it loses by swimming with its mouth open) is approximately 4×10^3 copepods m^{-3}. It is also reasonably consistent with Wishner *et al.*'s (1995) observations for the entire MOCNESS data set from all SCOPEX cruises of a minimum peak copepod abundance of 1.0×10^3 copepods m^{-3} in 1988 and 9.7×10^3 copepods m^{-3} in 1989 in areas where right whales were feeding.

The mean and peak copepod concentrations observed around Whale A during tow-yo 5 were 8.7×10^3 and 4.1×10^4 copepods m^{-3}, respectively. If we assume the mean energy value of each copepod is about 10^{-3} kcal, then the mean energy intake of Whale A during this period was roughly 3.8×10^4 kcal h^{-1} (assuming a swimming speed of 1.2 m s^{-1} and a mouth area of 1 m^2). At this rate, a whale would have to feed for approximately 5.5 h just to satisfy its daily basal metabolism energy requirement of 2.1×10^5 kcal (Kenney *et al.*, 1986). Up to five times this amount may be required to sustain active metabolism and feeding (Kenney *et al.*, 1986). It therefore seems that right whales must find even denser concentrations of copepods if they are to survive in the long term, especially since any food a right whale eats during the summer must provide it not only with its daily energy requirement but also with additional energy it will need for growth, reproduction, and metabolism during the winter migratory period (duration not known, possibly as long as 3–5 months) when it may not feed at all.

Denser concentrations of copepods are available in the GSC. The morning after tow-yos 5 and 6, Stars was found to be skim-feeding on a *Calanus finmarchicus* patch in which a bucket sample gave a concentration of 3.3×10^5 copepods m^{-3}. If this one sample approximated the mean concentration of this patch (or of the areas of the patch in which Stars fed), then Stars had a mean energy intake of 1.4×10^6 kcal h^{-1}. At this rate, she could consume her daily basal metabolic energy requirement in approximately 9 min, and her annual requirement in approximately two days (assuming continuous feeding). Clearly, seeking out and exploiting the densest copepod patches or maximum densities within larger patches would be an energetically optimal foraging strategy for right whales. Based on photographic observations made from the submersible *Delta* in the GSC region in June 1987, Wishner *et al.* (1995) report maximum copepod concentrations of up to

1.6×10^6 copepods m^{-3} in thin layers at depths near 16 m. Within right whale feeding areas in Cape Cod Bay, Mayo and Goldman (1992) showed variation of several orders of magnitude in zooplankton density over distances of only 10–15 m, with peak densities within "micro-patches" as high as 3×10^6 copepods m^{-3}, an order of magnitude higher than our densest sample.

Leising (1994) recently described some laboratory observations of copepod swarming which suggest that individual copepods attempt to "maintain a personal space only slightly larger (1.2–1.3 times) than their own body dimensions". This suggests that a crude estimate of the maximum copepod concentration that could have occurred during our June 1989 SCOPEX observations was

$$C_{\max} = \frac{1.41}{(NND_{\min})^3} = 1.3 \times 10^7 \text{ copepods m}^{-3}$$

where the minimum, nearest-neighbor distance $NND_{\min}$ in mm is estimated from the average antenna length ℓ using

$$NND_{\min} = 2.45\ell - 0.21,$$

(A. Leising, personal communication, 1995). The average antenna length is assumed equal to the average cephalotorax length (see Fig. B2 caption, Appendix B), so that $\ell = 2.0$ mm and $NND_{\min} = 4.7$ mm. The resulting value of $C_{\max}$ is roughly 40 times the bucket sample concentration. The average spacing between individual copepods in the bucket sample was only 16 mm, contributing to the reddish hue of the sample and the patch in the ocean.

One objective of SCOPEX was to examine several hypotheses about what processes might cause the formation of such dense copepod aggregations in late spring in the northern Great South Channel region (Kenney and Wishner, 1995). Three hypotheses were initially advanced. The advection hypothesis states that an interaction between the water flow and the behavior of the copepods (especially vertical migration and a preference for some depth band) passively concentrates the copepods. The productivity hypothesis states that the high copepod concentrations are due to high primary productivity in the area (i.e. a simple food chain response). The social behavior hypothesis states that a species-specific social behavior (e.g. swarming) creates the dense copepod aggregations.

Wishner *et al.* (1995) found that in the two years (1988 and 1989) during SCOPEX, the densest copepod aggregations were found near the front of the surface fresh water plume east of Cape Cod, suggesting that regional advection was important. Epstein *et al.* (1993) have examined CTD and acoustic biomass data collected on the same *Endeavor* SCOPEX'89 cruise in a small-scale frontal feature in the surface plume, and suggested that the horizontal convergence associated with surface subduction, coupled with the copepods' tendency to maintain their depth near a fixed level near the surface, could explain a significant increase in the local near-surface copepod concentration. Thus, differential advection on regional and smaller scales, coupled with a specific copepod behavior, appear to be important processes in this region. Durbin *et al.* (1995) found no evidence of localized higher primary productivity to support the productivity hypothesis. Since the biological and physical data reported in this paper do not suggest that the small-scale subduction concentration mechanism suggested by Epstein *et al.* (1993) was active either during or immediately prior to the measurements made on 3–4 June, we conclude that some non-physical, species-specific animal behavior (such as swarming or some other unknown

physical mechanism) must be partially responsible for creating the very densest copepod patches observed during SCOPEX.

Acknowledgements—We want to thank the many individuals who helped to make SCOPEX a successful field experiment. In particular, we want to acknowledge the encouragement and strong support of H. Winn, who served with K. Wishner as SCOPEX co-coordinators; P. Wiebe, who provided valuable input concerning the interpretation of acoustic data; A. and E. Durbin, who kindly shared their measurements of copepod size and energy content; A. Leising, who shared his unpublished results on copepod swarming; the comments of two reviewers who helped improve the manuscript, and the crews of the R.V.s *Endeavor* and *Marlin*.

The SCOPEX field work reported here was supported by the National Science Foundation and the U.S. Department of Interior Minerals Management Service through NSF grants OCE 87–13988 and OCE 91–01034 to R. Beardsley and C. Chen, grants OCE 87–11847 and OCE 89–15610 to K. Wishner, grants OCE 87–11851 and OCE 89–15610 to R. Kenny, and grants OCE 89–40247 and OCE 89–15844 to M. Macaulay. Support for A. Epstein during the analysis phase of this work was provided by the National Oceanic and Atmospheric Administration under Grant NA36GP0374. The final preparation of this manuscript was supported by NSF under grants OCE 93–15713 and OCE 93–13671 with help from J. Cook and A.-M. Michael. This is WHOI contribution no. 8908 and U.S. GLOBEC contribution no. 65. The U.S. GLOBEC program is funded jointly by NSF and NOAA.

REFERENCES

Burd B. J. and R. E. Thomson (1993) Flow volume calculations based on three-dimensional current and net orientation data. *Deep-Sea Research I*, **40**, 1141–1153.

Cetacean and Turtle Assessment Program (CETAP), (1982) A characterization of marine mammals and turtles in the Mid- and North-Atlantic areas of the U.S. outer continental shelf, final report. Contract no. AA551-CT8-48. Bureau of Land Management, U.S. Dept. of the Interior, Washington, DC, 586 pp. (NTIS no. PB83-215 855).

Chen C., R. C. Beardsley and R. Limeburner (1995a) Variability of water properties in late spring in the northern Great South Channel. *Continental Shelf Research*, **15**, 415–431.

Chen C., R. C. Beardsley and R. Limeburner (1995b) Variability of currents in late spring in the northern Great South Channel. *Continental Shelf Research*, **15**, 451–473.

Comita G. W., S. M. Marshall and A. P. Orr (1966) On the biology of *Calanus finmarchicus*, XIII. Seasonal change in weight, calorific value and organic matter. *Journal of the Marine Biological Association of the U.K.*, **46**, 1–17.

Durbin E. G. and A. G. Durbin (1983) Energy and nitrogen budgets for the Atlantic menhaden, *Brevoortia tyrannus* (Pisces: Clupeidae), a filter-feeding planktivore. *Fishery Bulletin*, **81**, 177–199.

Durbin E. G., R. G. Campbell, S. L. Gilman and A. G. Durbin (1995) Diel feeding behavior and ingestion rate in the copepod *Calanus finmarchicus* in the southern Gulf of Maine during late spring. *Continental Shelf Research*, **15**, 539–570.

Epstein A. W., R. C. Beardsley and M. C. Macaulay (1993). Mechanisms of flow-induced aggregation and concentration of zooplankton at fronts. Larval Ecology Meetings; Stony Brook, NY, August, 1993.

Gaskin D. E. (1987) Updated status of the right whale *Eubalaena glacialis*, in Canada. *Canadian Field-Naturalist*, **101**, 295–309.

Gaskin D. E. (1991) An update on the status of the right whale *Eubalaena glacialis*, in Canada. *Canadian Field-Naturalist*, **105**, 198–205.

Kenney R. D. and K. F. Wishner (1995) The South Channel Ocean Productivity Experiment. *Continental Shelf Research*, **15**, 373–384.

Kenney R. D., M. A. M. Hyman, R. E. Owen, G. P. Scott and H. E. Winn (1986) Estimation of prey densities required by western North Atlantic right whales. *Marine Mammal Science*, **2**, 1–13.

Kenney R. D., H. E. Winn and M. C. Macaulay (1995) Cetaceans in the Great South Channel, 1979–1989: Right Whale (*Eubalaena glacialis*). *Continental Shelf Research*, **15**, 385–414.

Leising A. W. (1994). The personal space of copepods. *Eos Transactions, American Geophysical Union*, **75**(3), 195 (abstract).

Macaulay M. C., K. F. Wishner and K. L. Daly (1995) Acoustic scattering from zooplankton and micronekton in relation to a whale feeding site near Georges Bank and Cape Cod. *Continental Shelf Research*, **15**, 509–537.

Matthews L. H. (1938) Notes on the southern right whale *Eubaleana australis*. *Discovery Reports*, **17**, 169–182.
Mayo C. A. and L. Goldman (1992). Right whale foraging and the plankton resources in Cape Cod and Massachusetts Bays. In: *The right whale in the western North Atlantic: A science and management workshop*. J. Hain, editor, NEFSC Ref. Doc. 92–05. National Marine Fisheries Service, Northeast Fisheries Science Center, Conservation and Utilization Division, Woods Hole, MA, pp. 43–44 .
Mayo C. A. and M. K. Marx (1990) Feeding behavior of northern right whales, *Bubalaena glacialis*, in Cape Cod Bay, and associated zooplankton characteristics. *Canadian Journal of Zoology*, **68**, 2214–2220.
Murison L. D. and D. E. Gaskin (1989) The distribution of right whales and zooplankton in the Bay of Fundy, Canada. *Canadian Journal of Zoology*, **67**, 1411–1420.
Nemoto T. (1970) Feeding patterns of baleen whales in the ocean. In: *Marine food chains*, J. H. Steele, editor, University of California Press, Berkeley, CA, pp. 241–252.
Omura H., S. Ohsumi, T. Nemoto, K. Nasu and T. Kasuya (1969) Black right whales in the North Pacific. *Science Report of the Whales Research Institute*, **21**, 1–96.
Pivorunas A. (1979) Feeding mechanisms of baleen whales. *American Scientist*, **67**, 432–440.
Schoenherr J. R. and K. F. Wishner (1990). Abundance and distribution of the copepod *Calanus finmarchicus* in the Great South Channel (MOCNESS tows). Final Data Report for EN-174, EN-176, and EN-196. Unpublished manuscript.
Scott G. P., R. D. Kenney, R. E. Owen, M. A. M. Hyman and H. E. Winn (1985) *Biological and physical oceanographic correlative and to cetacean density distribution in the Great South Channel*. Document C. M. 1985/N:6/Ref. L. International Council for the Exploration of the Sea, Copenhagen, 36 pp.
Tomilin A. G. (1957). *Mammals of the U.S.S.R. and adjacent countries*, Volume IX, *Cetacea*. Translation no. 1124, Israel Program for Scientific Translation, Jerusalem (1967), 738 pp.
Watkins W. A. and W. E. Schevill (1976) Right whale feeding and baleen rattle. *Journal of Mammals*, **57**, 58–66.
Watkins W. A. and W. E. Schevill (1979) Aerial observation of feeding behavior in four baleen whales: *Eubalaena glacialis, Balaenoptera borealis, Megaptera novaeangliae*, and *Balaenoptera physalus*. *Journal of Mammals*, **60**, 155–163.
Wiebe P. H., K. H. Burt, S. H. Boyd and A. W. Morton (1976) A multiple opening/closing net and environmental sensing system for sampling zooplankton. *Journal of Marine Research*, **34**, 313–326.
Wiebe P. H., A. W. Morton, A. M. Bradley, R. H. Backus, J. E. Craddock, V. Barber, T. J. Cowles and G. R. Flierl (1985) New developments in the MOCNESS, an apparatus for sampling zooplankton and micronekton. *Marine Biology*, **87**, 313–323.
Winn H. E., J. D. Goodyear, R. D. Kenney and R. O. Petricig (1995) Dive patterns of tagged right whales in the Great South Channel. *Continental Shelf Research*, **14**, 593–611.
Wishner K., E. Durbin, A. Durbin, M. Macaulay, H. Winn and R. Kenney (1988) Copepod patches and right whales in the Great South Channel off New England. *Bulletin of Marine Science*, **43**, 825–844.
Wishner K. F., J. R. Schoenherr, R. C. Beardsley and C. Chen (1995) Abundance, distribution, and population structure of the copepod *Calanus finmarchicus* in a springtime right whale feeding area in the southwestern Gulf of Maine. *Continental Shelf Research*, **15**, 475–507.

APPENDIX A

Intercomparison between 200 kHz acoustic data and MOCNESS biomass estimates

Figure 3A shows the zooplankton biomass field obtained from the 30 s, 200 kHz acoustic data during leg 1 of tow-yo 5, with the path of MOCNESS 43 superimposed. The acoustic biomass data are shown as a function of distance along the shiptrack (measured relative to the surface water) and depth to 25 m. The zero biomass shown in the top 4 m is an artifact of the blanking of acoustic data near the transducer. Figure 3A shows a dense, patchy layer of copepods lying above a much denser and thicker layer of larger zooplankton centered near 20 m. This deeper zooplankton layer was also prominent in the 120 kHz acoustic data, and the dominant species was identified by Macaulay *et al.* (1995) as euphausiids (*Meganyctiphanes* sp.). The mean copepod biomass between 4 and 10 m is about 6 g m^{-3}, while the larger zooplankton layer below the copepod layer has a maximum mean "biomass" of about 440 g m^{-3} at 20 m. (The large value of this number indicates the presence of some organism other than copepods, but it does not represent an actual estimate of biomass for that organism, since the conversion factor of -36 dB kg^{-1} is valid only for copepods.)

Whale A appeared to be feeding within the top 10 m of the water column, and so the MOCNESS was set to sample horizontally between 8 and 11 m after an initial oblique tow from the surface to 8 m (net no. 1). Although

Table A1. *Table of correlation coefficients between MOCNESS* 43 (*nets* 2–9) *and the* 30 s 200 kHz *biomass estimates listed as a function of time and depth shifts between the two data sets. The time and depth increments used are* 30 s *and* 1 m. *The best correlation occurred with a time shift of* 60 s *and a depth shift of* 1 m. *The MOCNESS net* 1 *biomass datum is not included in this comparison since it was obtained on an oblique tow from the surface through a near surface layer not sampled with the* 200 kHz *system.*

Δt (sec) \ Δz (m)	0	1	2
0	0.63	0.68	0.26
30	0.88	0.94	0.71
60	0.90	0.97	0.76
90	0.88	0.96	0.74
120	0.84	0.94	0.71

the average biomass measured during MOCNESS 43 was 6.2 g m^{-3}, essentially identical to the mean 5–10 m acoustic estimate, the two data sets must be aligned carefully before additional comparison because of the large spatial variation in copepod biomass apparent in Fig. 3A and Table 2.

The MOCNESS pressure sensor was not very accurate (showing a pressure offset of as much as 5 m at the sea surface before and after these tows), and the depth at which the acoustic fin was towed is not known precisely; in addition, the MOCNESS and acoustic systems used different PC clocks for data acquisition and were towed from different positions on the ship with different amounts of wire out. To compensate for these factors, we chose to shift the MOCNESS biomass data in time and depth relative to the acoustic biomass data to find the best correlation. The sensitivity of the correlation coefficient to this shifting is shown in Table A1. The best fit occurs with a time shift of 60 s (two acoustic time bins) and a depth shift of 1 m (one acoustic depth bin); these values are reasonable considering the relative positions of the acoustic fin and MOCNESS and the low tow speed. Figure B1 shows the MOCNESS data plotted against the biomass values the MOCNESS would have found if it had sampled the acoustic field as shown in Fig. 3A (with the optimal shift). The agreement is quite good, with a correlation coefficient equal to 0.971, significantly different from zero above the 99.9% level. The linear regression slope is 0.68 ± 0.17 (95% confidence limit), suggesting that the 200 kHz system may tend to underestimate copepod biomass at the larger values in this application, although more samples are needed to substantiate this suggestion. The overall good agreement between the MOCNESS and 200 kHz biomass estimates in this comparison seems due in part to the fact that the zooplankton population being sampled in the top 10 m was almost entirely a mixture of two stages (CIV and CV) of a single copepod species (*Calanus finmarchicus*) (Table 2).

This comparison gives confidence that the 200 kHz system was measuring *Calanus* biomass accurately on small scales when processed in 30 s blocks with optimal settings. Note how even the individual MOCNESS samples can average over some of the smaller peaks and holes in the acoustic biomass field shown in Fig. 3A, making a continuous acoustic record very valuable in determining small-scale variations in biomass.

APPENDIX B

Comparison between light transmission and 200 *kHz biomass estimates*

The optical characteristics of pure seawater depend only weakly on temperature, salinity and pressure, so that variations in the light tramsmission of water in the ocean are caused primarily by the presence of organisms, their waste products, and other particulate material. During the CTD sampling conducted near Whale A and Stars, we observed significant scatter in light-transmission profiles in the upper 30–40 m of the water column which we believe to have been caused by individual copepods. The following simple argument attempts to quantify the process by which the presence of copepods could attenuate a transmissometer light beam.

Suppose the light beam from the transmissometer's source to its receiver is a cylinder of radius R and length L. If we model the copepods as opaque cylinders of radius r and length h, then the percentage of the beam light that is blocked by copepods, assuming that the copepods are spaced far enough apart that their shadows do not overlap, is

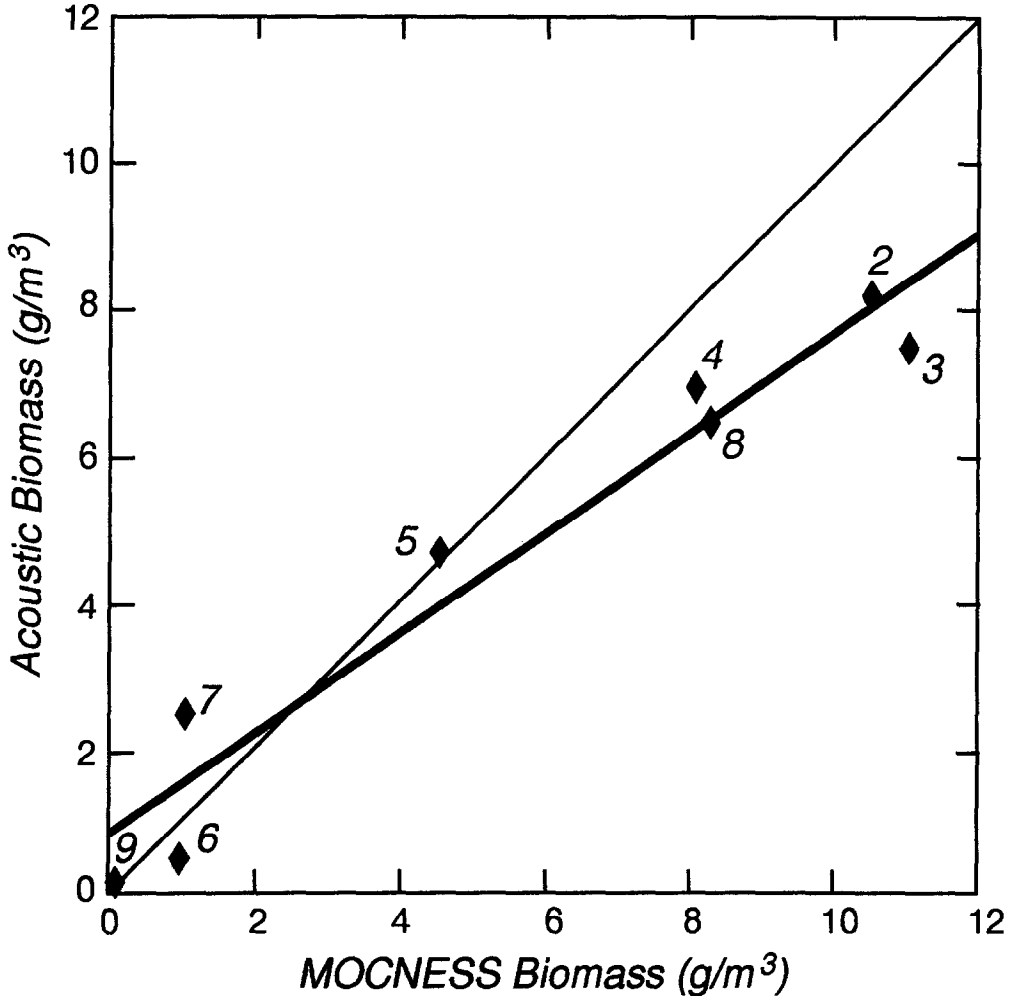

Fig. B1. Comparison of the MOCNESS 43 biomass estimates with the biomass estimates the MOCNESS would have measured if it had sampled the 30-s, 200-kHz biomass field shown in Fig. 3A along the path that gives the best correlation between acoustic and MOCNESS data. The number at each value indicates the net number. Net 1 is not used since its oblique sample included the top 4 m, where no acoustic data were taken. The slope of the least-squares best-fit line (heavy) through the data is 0.69 ± 0.17: a perfect comparison would have a slope of 1 (light).

given by

$$B_z = 100\% \times (N_z 2rh)/(\pi R^2),$$

where N_z is the number of copepods in the beam's path. N_z is related to the concentration of copepods C_z by

$$N_z = C_z \pi R^2 L,$$

so that the percentage of light blocked is given by

$$B_z = 100\% \times C_z 2rhL.$$

For $L = 25$ cm, the percentage of light blocked versus copepod concentration is plotted in Fig. B2 for *Calanus finmarchicus* copepodite stages CIV and CV. This figure shows, for example, that for CIV, a concentration of

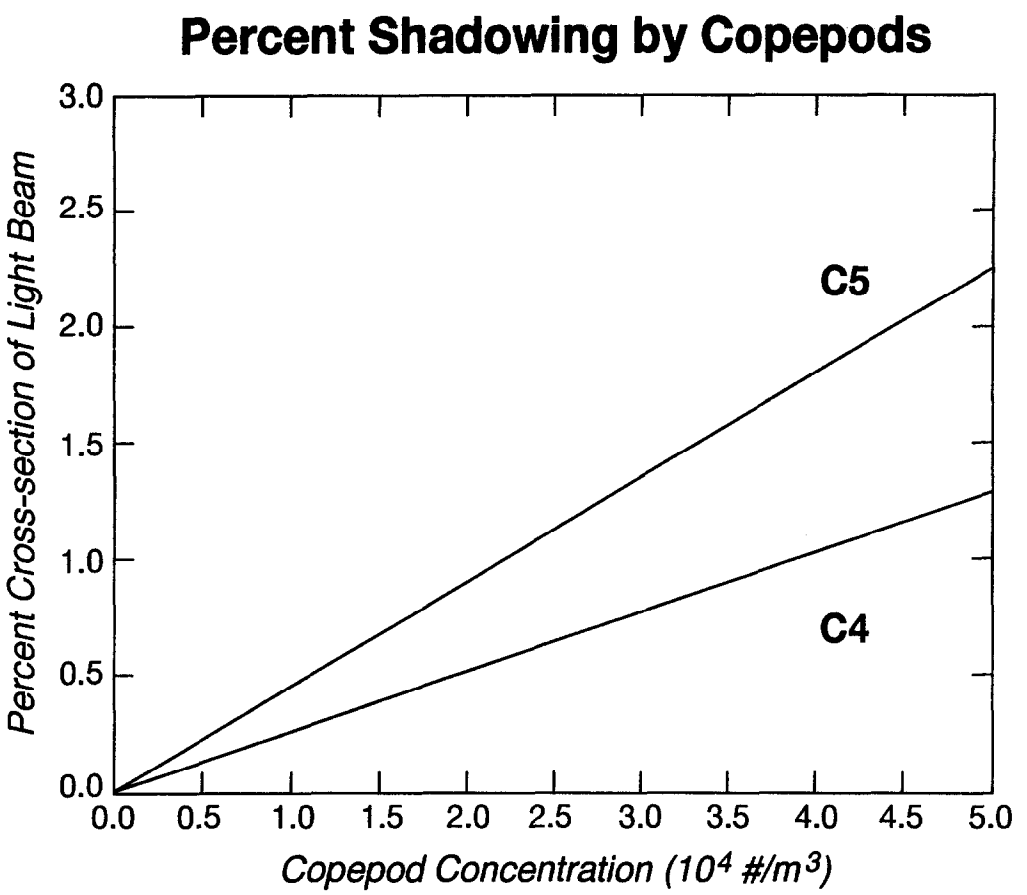

Fig. B2. The per cent cross-section of the transmissometer light beam that would be blocked as a function of copepod concentration for stages CIV and CV *Calanus*. To construct this figure, the copepod is modeled as a cylinder of length L_c and width $0.43 \times L_c$ where L_c is the cephalothorax length. A. and T. Durbin (personal communication, 1995) report mean values of L_c of 1.75 mm for stage CIV and 2.28 mm for stage CV based on measurements of the surface *Calanus* population during the May–June SCOPEX'89 *Endeavor* cruise.

3.8×10^4 copepods m^{-3} would reduce the amount of light transmitted by 1%. In the light-transmission profile shown in Fig. B3A, reductions as large as 1.5% are seen near 7 and 14 m. If we assume that the composition of the copepod patch sampled in Fig. B3A is similar to that found in the MOCNESS 43 tows, i.e. that the patch is roughly 42% CIV and 58% CV, then a 1.5% reduction in transmitted light implies a copepod concentration of 4.1×10^4 copepods m^{-3}. This is about 1.7 times the maximum concentration found during MOCNESS 43. At this concentration, about three copepods would be in the light beam on average, which suggests that the assumption that their shadows do not overlap is reasonable.

To further examine the hypothesis that scatter in the transmissometer data was due to obstruction of the light beam by copepods, we compared the scatter with 200 kHz acoustic biomass estimates made at the same time. For each light-transmission profile, we subjectively drew a smooth curve to fit the maximum light transmission profile (on the assumption that this "background" profile would have matched most data points if not for the presence of copepods—see the example in Fig. B3A). We then subtracted the raw data from this background profile to determine the deviation of the observed light transmission from the background, and calculated the root mean square (rms) deviation in 1 m depth bins. We then compared the rms deviation profiles to the contemporaneous 200 kHz biomass profiles obtained during leg 1 of tow-yo 5 over the upper 25 m, where we believe the acoustic instrument was observing primarily copepods.

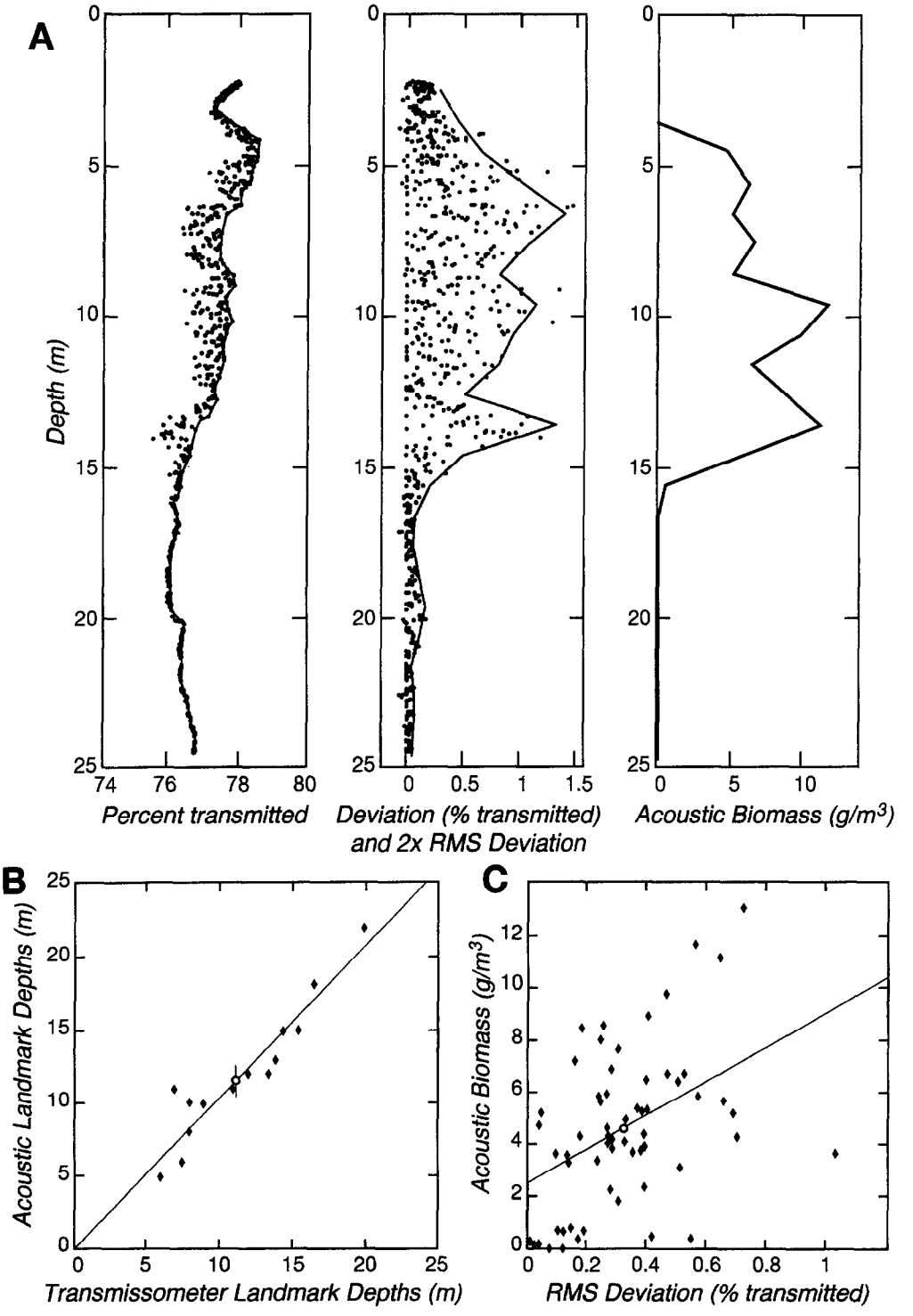
A
Depth (m)
0
5
10
15
20
25
74
76
78
80
Percent transmitted
0
0.5
1
1.5
Deviation (% transmitted) and 2x RMS Deviation
0
5
10
Acoustic Biomass (g/m3)
B
Acoustic Landmark Depths (m)
Transmissometer Landmark Depths (m)
C
Acoustic Biomass (g/m3)
RMS Deviation (% transmitted)

As in the comparison between MOCNESS and acoustic data, we shifted the nominal depth of the acoustic data relative to that of the transmissometer data in order to account for uncertainty in the depth at which the acoustic system was deployed. The best correlation between acoustic and transmissometer data was given by a depth offset of 1 m (one acoustic depth bin). No time adjustment was necessary. (This offset, as well as the additional 1 m and 60 s offsets between MOCNESS and acoustic data are taken into account in Fig. 3A). Figure B3B plots the depths at which major features such as distinct peaks or the sharp drop-off of intensity at the base of the copepod layer occur in the acoustic data versus the depths at which they occur in the transmissometer data. The two data sets correspond very well in this qualitative sense, with a correlation coefficient of 0.945, significantly different from 0 at the 99.9% level. This qualitative agreement between rms transmissometer deviation and acoustic biomass estimate is illustrated in Fig. 3B, where vertical profiles of the two quantities are compared.

The data do not correspond as well in a quantitative sense. Figure B3C shows the acoustic biomass estimate for each depth bin plotted versus the rms transmissometer deviation for the corresponding bin. The correlation coefficient 0.442 is significantly different from 0 at the 99.9% level, but the correlation is too weak to make it possible to use transmissometer data to predict biomass with much confidence. This is not unreasonable, given the patchiness of the copepod distribution (as shown in the acoustic data) and the large differences between the water volumes sampled with the two instruments. The acoustic profiler integrates, for 30 s, backscatter data from a relatively wide field (the size of which depends on the depth bin), while the transmissometer samples only the small volume within the light beam path for 2–3 s over a 1 m depth bin.

Fig. B3. (A) Raw profile of per cent light transmission versus depth at cast 2 of tow-yo 5 (left panel). The curve connecting the maximum transmission represents the putative background profile. Profile of percent light-transmission deviation, i.e. the difference between the raw values and the background profile (center panel). The solid line represents twice the rms deviation calculated for 1-m bins. Profile of 30 s, 200 kHz acoustic biomass corresponding to station 2 (right panel). (B) Scatterplot of "landmark" depths (the depths of major qualitative features) in light-transmission deviation versus those in the acoustic biomass data. Slope of best-fit line through the origin is 1.04 ± 0.21 (95% confidence). (C) Scatterplot of rms light transmission deviation versus acoustic biomass. Best fit line has correlation coefficient 0.44, which is significant above the 99.9% level. Data shown are from all profiles where comparison is possible.